A Monte Carlo Simulation of the Aggregation, Phase-Separation, and Gelation of Model Globular Molecules

Geoffrey Costello and Stephen R. Euston*

School of Life Sciences, Heriot-Watt University, Riccarton, Edinburgh EH14 4AS, UK

Received: November 1, 2005; In Final Form: March 22, 2006

Monte Carlo computer simulation on a square 3-D lattice is used to model state behavior of globular copolymers. Two types of globular molecules were defined. One consisted of a single type of subunit (a homopolymer) while the second contained a core of strongly attractive subunits and an outer layer of less strongly attractive subunits (a heteropolymer). Systems of globules were simulated at varied volume fraction (V_F) and reduced temperature (T_R), and state diagrams were constructed. These state diagrams contained state boundaries defined by the V_F/T_R combinations at which the system formed a percolating network and at which the various component subunits in the globule unfolded. Simulated systems could exist in a number of states (between 4 and 7), depending on the V_F, T_R, whether the molecule was a homo- or heteroglobule and whether the globules were allowed to interact with each other or not. All systems exhibited a gelation/crossover line that resembled a lower critical solution temperature. All systems also exhibited a critical gelation concentration, above which a continuous network was formed. The critical gelation concentration varied between about 2−4% V_F depending on the type of system. This is comparable to experimental critical gelation concentrations of in the region of 4% (w/w) for a range of associating polymers and biopolymers such as globular proteins and polysaccharides. Other states were formed which included one where elongated, fibril-like aggregated strands were formed, and a micelle-like aggregated state. The results are discussed in terms of the known state behavior of associating polymers and biopolymers (proteins and polysaccharides).

Introduction

The phase behavior of polymers and biopolymers in particular is very complex and only partially understood.[1−3] Polymer solutions can exist in a number of different thermodynamically or kinetically stable states depending on the temperature, volume fraction, composition of the aqueous phase, and the nature of the interactions between the polymer molecules. These include solutions and gelled and phase-separated states, the latter two consisting of aggregated molecules. In biopolymer systems, e.g., protein and polysaccharides, the gelled state is common and is utilized, for example, in many manufactured foods to give products a solid-like structure. Phase-separated states have, until recently, been less common in food systems, although now the properties of phase-separated biopolymer mixtures are being investigated as potential novel texturants.[4]

Tanaka[5] has defined associating polymers as polymer chains that are capable of forming weak bonds that can be formed and broken by thermal motion. Associating polymers can form a number of different phases depending on the temperature and polymer concentration. Moreover, transitions between these phases are reversible by changing temperature and concentration. Telechelic polymers are the simplest associating polymers, which have a single associating group at each end of the molecule. These are capable of forming a number of different association structures in solutions, including intramolecular loops, flower micelles, and compact micelles where polymers are shared between different micelles.[6−8] Block copolymers that consist of hydrophobic and hydrophilic blocks are known to self-associate into micellar structures under the appropriate conditions of temperature and polymer concentration.[1,2] They have also been observed to form complex mesophases at higher concentrations, including hexagonal, cylindrical, and lamellar phases.[1,2] Biopolymers are an example of associating polymers and share some features of the state behavior of synthetic associating polymers. Some proteins, such as the milk caseins, can be described as block copolymers on a coarse-grained mesoscopic level,[9,10] and these too display temperature and concentration dependent micellization behavior,[11,12] with loop, flower-like, and compact micellar forms reproted. They have not been observed to form more complex mesophases, and this may be due to the difficulty in making the highly concentrated protein solutions where this may occur.

A second type of association structure formed in associating polymer/biopolymer solutions is a gel. Globular protein gelation and gel structure have been studied for many years,[3] and much is known about the kinetics[3,13] and the relationship between structure and texture[14] from an experimental point of view. Despite this large body of knowledge, there are still some structural aspects of globular protein gels that are not well understood. One example is the ability of globular proteins such as β-lactoglobulin to form vastly different gel structures under different solvent conditions.[15−17] Under conditions of high electrostatic repulsion (low ionic strength, low pH well away from the proteins pI), the proteins aggregate in a linear fashion to form fine filaments or fibrils[15] with a radius approximately the same as that of a single protein molecule. At a high enough protein concentration the fibrils join together to form a transparent gel. Increasing the ionic strength at low pH leads to a change in structure to shorter less flexible clusters. At pH 7, above the pI, stranded gels are still formed but the radius of the strands

* Corresponding author. Tel.: +44 131 4513640. Fax: +44 131 4513009. E-mail: s.r.euston@hw.ac.uk

10.1021/jp056304v CCC: $33.50
Published on Web 05/02/2006

suggests they are several protein molecules thick and are thus much coarser. There is evidence that fibril formation involves the formation of intramolecular β-sheet structures.[18] More recent evidence suggests that these fibrils may not be the end-point of aggregation and a semicrystalline spherulite phase has been observed to form from fibrils under some conditions.[19] At ionic strength and/or pH close to pI where electrostatic repulsion is weak due to charge screening, a densely packed, opaque particulate gel is formed. This may represent a demixed or phase separated state.[13]

The third type of association structure or aggregated state is the phase-separated state. These occur when polymers associate without forming a continuous gelled network, but separate into a polymer-rich and solvent rich-phase. Two mechanisms of phase-separation have been identified, nucleation and growth and spinodal decomposition,[20,21] which occur on either side of the spinodal line separating unstable and metastable regions in the phase diagram. Phase separation occurs because association of the polymers, and the subsequent demixing leads to a decrease in the free energy of the system. For this to occur in a polymer solution or polymer mixtures, fluctuations in the local polymer concentration must occur which lead to polymer-rich phases that grow with time. In the metastable region, small concentration fluctuations are suppressed since they increase the free energy, and only concentration fluctuations above a certain critical size will decrease the free energy and allow phase-separation. This is the nucleation and growth mechanism, and it is characterized by a system where the phase-separated polymer forms as a pure phase, has an uneven distribution through the system, and the size distribution of the separating regions is broad. Spinodal decomposition, on the other hand, occurs in the unstable region of the phase diagram. In the unstable region, large concentration fluctuations grow slowly due to long diffusion times for the polymer, and small concentration fluctuations also grow slowly. In spinodal decomposition there is an intermediate concentration fluctuation that grows at the fastest rate, and this dominates the phase separation mechanism. As a result, spinodal decomposition is characterized by initially evenly spaced, separated domains. Phase separation is complicated further by the possibility of a coupling of gelation and phase separation that can trap the phase-separated structure in a transient or persistent gel.[22−27]

In contrast to the experimental study of gel structures, Clarke et al.[13] have pointed out that the theoretical description of these processes is lacking. Clarke et al.[13] have themselves proposed a mean-field model incorporating a nucleation and growth mechanism for fibril formation. The model is only partially successful at describing the gelation of acidified β-lactoglobulin solutions. In particular, it appears that mathematical modeling has difficulty in describing phase-separated gel states. Clarke et al.[13] conclude that simulation may be a better route to study the details of gel structure.

In this study we introduce a simple model for globular molecules that allows us to simulate them as an assembly of connected spheres (subunits). This model we call the deformable globule model, and we have used this previously to successfully simulate the adsorption and unfolding of globular molecules at surfaces.[28] By controlling the attractive interactions between subunits we allow the molecule to fold or unfold. Thus the molecule is able to undergo an order−disorder transition between compact, folded and disordered, unfolded states of the molecule. Moreover, it is possible to define different types of subunits that can interact in different ways with other subunits in the same globule or on different globules, and here we will present results for both a homoglobule and heteroglobule containing two subunit types. We will show that it is possible to use this model to simulate the state behavior of systems of model globular molecules. Our eventual goal is to simulate globular protein state behavior and gelation. This is a complex task because of the structural complexity of protein molecules, and because they change their structure and association/aggregation behavior in response to external factors such as pH and ionic strength. In the past, few detailed simulations that incorporate all of these factors have been attempted, and not in the context of protein gel formation and structure. Nor has there been any real attempt previously to incorporate a representation of the globular nature of proteins into simulations. Thus, it is relevant for us to first introduce a minimalist model for globular protein-like molecules prior to developing a more complex, detailed model. The rationale behind this is that with a highly simplified model, we can investigate features of the state behavior and gelation behavior that arise solely from the globular character of the molecules, in the absence of complicating factors that would need to be incorporated into a more complex protein model. This model is perhaps closer to that of linear homopolymers and copolymers rather than proteins, although it does have some relevance to the latter. Therefore, we will discuss the results of this model in the context of polymeric solutions, while drawing analogy with relevant protein systems.

Simulation Methodology

Simulations were carried out on a cubic lattice with a constant number (125) of globules, and the side length of the box adjusted so as to vary the volume fraction (V_F) occupied by subunits of the globule. Periodic boundary conditions were defined in the *x*, *y*, and *z* coordinate directions. A globular molecule was simulated using a 3-D version[28] of the deformable globule model proposed originally by Dickinson and Euston.[29a−c] The protein is defined as a collection of individual subunits, with 64 chosen for most of this work. Each subunit occupies a single lattice site. The subunits in a globule are not bound to each other in a linear chain via fixed bonds. Instead they are held together by nonbonded attractive interactions between each subunit. Three different types of subunit movement are allowed. (a) A subunit is chosen at random and an attempt is made to move this into one of the 26 lattice sites in the nearest neighbor shell around that subunit. This movement routine is implemented at each Monte Carlo attempt. (b) A globule is chosen at random and an attempt is made to move, sequentially, each subunit into a randomly chosen vacant adjacent lattice site. As well as allowing for limited diffusion of the globule around the simulation box, this algorithm also allows for substantial shape changes in the globule. This movement routine is implemented every 50 Monte Carlo attempts. (c) A particle is chosen at random and a constant random displacement of $\pm$ 1 lattice site is applied in each of the *x*, *y*, and *z* coordinate directions. This algorithm is better for whole globule displacement, but does not lead to globule shape change. This algorithm is inefficient when the globule radius of gyration is large or when the volume fraction is high. This movement routine is implemented every 50 Monte Carlo attempts.

The movement of subunits is accepted according to the following criteria. (i) The excluded volume principle is applied (i.e., double occupancy of a lattice site does not occur). (ii) Importance sampling is used to test the energetic favorability using the Metropolis form of the Monte Carlo method. (iii) Connectivity of all subunits in the globule is maintained. This condition is tested using an algorithm for testing particle connectivity in aggregates.[30]

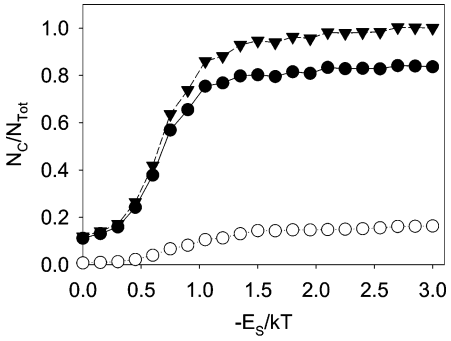

Figure 1. Global unfolding curves for heteroglobules at $V_F = 2\%$. The normalized number of native contacts N_C/N_{Tot} is plotted against ϵ_s^{type1} for (▼) all subunits; (●) type 1 subunits; (○) type 2 subunits. Unfolding temperature is defined as the points of inflection of the curves.

Two types of globule were defined in this work. Molecules were represented either as a homoglobule, where there was only one type of subunit (type 1), or a heteroglobule with two types of subunit (type 1 and type 2). For the heteroglobule, the initial starting conformation was defined such that the type 2 subunits were clustered together at the core of the globule. These subunits were allowed to interact more strongly with each other than were the type 1 subunits so that the heteroglobule has a three-state unfolding transition compared to a two-state transition for the homoglobule (Figure 1).

Subunits interact via a pairwise additive square well potential. Pairs of subunits are deemed to be interacting if the second subunit occupies one of the 26 lattice sites that are directly adjacent to the first. If the square well is made attractive, i.e., it has a negative value of energy in units of kT, then the magnitude of this attraction (the well depth, denoted by ϵ_s) can be used to control the structure of the globule. By varying the strength of the square well attraction the globule can adopt either a compact, folded structure (high attraction between subunits) or an open, unfolded structure (low attraction). At attractive square well depths between these two states the globule undergoes an unfolding transition (order−disorder transition). In simulations where a heteroglobule is used, the type 2 subunits interact with a value of kT that is 75% greater than that of the type 1 segments, i.e., the ratio $\epsilon_s^{type2}/\epsilon_s^{type1} = 1.75$. This is used as a convenient way of simulating a globule with a three-state denaturation. Our heteroglobule model might be considered as a crude representation of a molecule with a hydrophobic core and a hydrophilic corona of subunits. We recognize that our representation does not give the correct temperature dependence for hydrophobic interactions, which increase in strength with increasing temperature up to around 70 °C. However, the net overall unfolding behavior is not unrealistic and we believe that this justifies the simplifications made.

Since we are using units of kT to characterize our interaction energies, changes in interaction strength can be considered to be the equivalent of a change in temperature, and our unfolding transition can be considered to represent thermal denaturation. Thus a decrease in attractive ϵ_s is equivalent to a temperature increase. This can be used to define a temperature range over which unfolding occurs. In Figure 1 the number of nearest neighbor contacts per subunit summed over all subunits in the globule (N_c) is used as a measure of the compactness (or openness) of the globule. The normalized number of nearest neighbor (N_c/N_{tot}), where N_{tot} is the maximum number of contacts possible, is plotted against ϵ_s/kT. There is a rapid transition from a compact, folded conformation to an unfolded, open conformation over a narrow range of ϵ_s. We have defined the unfolding transition as the value of ϵ_s at which there is a point of inflection in the curve. For the overall unfolding transition (N_c includes both type 1 and type 2 subunits) this corresponds to the point at which half of the nearest neighbor shell is unoccupied. The value of ϵ_s at the unfolding transition ($\epsilon_{s,u}$) can be used as a normalizing factor in the construction of a reduced temperature (T_R) scale for unfolding, i.e.,

$$T_R = (\epsilon_{s,u})/\epsilon_s^{type1} \quad (1)$$

In practice we use the value of $\epsilon_{s,u}$ for an isolated globule as the normalizing factor, and the interaction energy for type 1 subunits as the temperature scale. On this temperature scale the unfolding transition occurs at a value of 1.0, with values less than 1 corresponding to folded states and values greater than 1.0 to open, unfolded states.

In simulations where attractive interactions between homoglobules are included, we note that plots of N_c vs ϵ_s indicate that individual globules are unfolded, while simulated conformations of these systems suggested that compact conformations are still present. In this situation more than one globule has become aggregated together. This allows localized unfolding of the globules, while maintaining a folded, aggregated conformation. Thus, we are able to define two unfolding temperatures for systems where interglobule attraction is allowed. A local unfolding temperature is defined according to eq 1 by plotting N_c vs ϵ_s for contacts within a single globule and averaged over all globules. This line corresponds to an apparent unfolding of individual globules as they merge to form a larger globule, but this is still below the temperature at which a fully unfolded conformation is formed. The interesting thing about this local unfolding transition is that it occurs at temperatures below the unfolding temperature for an isolated globule, implying that unfolding of the globules can be driven by increases in concentration as well as temperature. The second unfolding temperature, a global unfolding temperature can be defined by plotting N_c vs ϵ_s for all contacts (inter- and intraglobule) in the system. The latter unfolding transition corresponds to the temperature at which aggregates become unfolded and disordered. For heteroglobules it is possible to follow the unfolding of both the type 1 and type 2 subunits, and also to define global and local unfolding transition for both types of subunit (for an example of this see Figure 1).

Simulation runs were carried out at varied globule volume fractions (V_F) and temperatures (T_R). Starting conformations at each V_F were generated by placing the required number of globules in random positions on the lattice. Initially, each globule was defined as a $4 \times 4 \times 4$ square conformation on the lattice. Simulations were carried out from the random starting conformations and were heated directly to the required temperature. These simulations were equilibrated until a constant internal energy was achieved and then sampled for a further $15-25 \times 10^6$ MC attempts.

Different cases were considered for the interactions between subunits on different globules. For homoglobules, in one case, type 1 subunits on different globules were allowed to interact only through excluded volume effects, i.e., the interaction energy between subunits in different globules was zero. The second case allowed type 1 subunits on different globules to interact with an attractive energy equal to the subunit interaction (ϵ_s^{type1}) between subunits in the same globule. For heteroglobules, in one case type 1 subunits were allowed only to interact with subunits on other globules through excluded volume interactions, while type 2 subunits were allowed to interact with an attractive interaction equal to ϵ_s^{type2}. In the second case for heteroglobules

both type 1 and type 2 subunits were allowed to interact with attractive interactions equal to ϵ_s^{type1} and ϵ_s^{type2} respectively.

Sampling of the equilibrium state of the simulations involved calculation of a number of parameters relating to the structure of both the individual globules and any aggregates and the gelled state. The aggregate size distribution was calculated using an algorithm devised by Stoddard.[30] A simple definition for the concentration at which the globules formed a gel has been used in this work. We have defined the gelation concentration at a particular reduced temperature as the concentration at which a single aggregate was formed in the box. We recognize that this is not an unambiguous definition of a percolation transition. However, our results suggest that the number and size of aggregates changes very rapidly as we approach our definition of the gelation point, and that as a result the gelation line we define using this method is close to the percolation transition. In systems where there are no attractive interactions between separate globules a cross-linked gel cannot form. The concentration at which a continuous network is formed might not best be described as a gelation point. It more closely resembles the crossover concentration observed in, for example, polysaccharide solutions. This corresponds to the biomolecule chains starting to overlap each other (i.e., the crossover from the dilute to the semidilute regime) and is characterized by a rapid increase in viscosity with increasing biomolecule concentration above this point. Thus, for systems where there are no interglobule interactions we will identify the T_R/V_F combinations at which a continuous network forms as a crossover concentration line, whereas in systems where interglobule interactions are allowed we will identify this line as a gelation line.

The system was further characterized by calculating the fractal dimension. The fractal dimension (d_f) was calculated using a mass fractal approach. In this method the number of subunits or globules ($N(r)$) a distance r from a given subunit or globule was derived and the fractal dimension calculated from the relationship

$$r \sim N(r)^{1/d_f} \tag{2}$$

$N(r)$ was calculated by averaging over the positions of all subunits/centers of mass. Two fractal dimensions were calculated, with one probing the correlation between the centers of mass of all subunits, and the second the correlation between the positions of all subunits. The structure of the gelled state was further characterized by calculating the accumulative void exclusion probability ($E(R)$), as suggested by Dickinson.[31] This calculates the probability that a particle of radius R is able to fit into a void in the simulation cell when it is randomly inserted into the cell. This parameter is related to the pore size distribution within the gel.

Results

State Diagrams and Conformations of Homoglobule Systems. Figure 2 shows the reduced unfolding temperature ($T_{R,u}$) for isolated homoglobules of differing size (number of subunits). Here the unfolding temperature has been normalized with respect to the unfolding temperature of the smallest globule simulated ($N = 27$). As the globule size increases, $T_{R,u}$ increases. Smaller values of the attractive ϵ_s are required to compensate for conformational entropy because of the cooperative effect of a larger number of interactions holding the structure together. We will see later that this dependence of $T_{R,u}$ on globule size impacts on the apparent globule unfolding temperature in systems where the individual globules are attracted to each other.

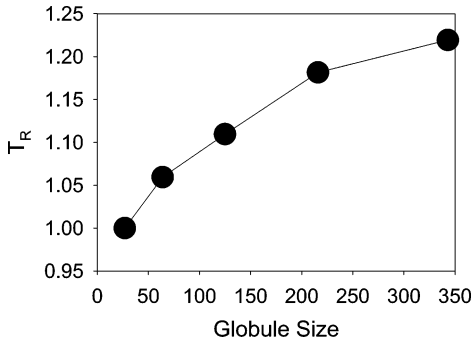

Figure 2. Dependence of reduced denaturation temperature on number of subunits in globule.

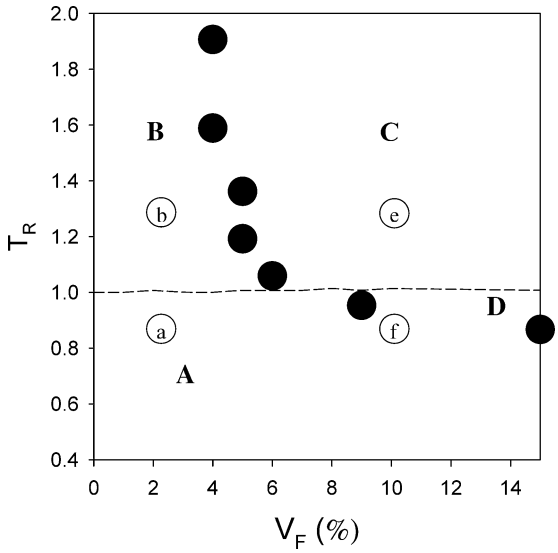

Figure 3. State diagram for homoglobules with no interglobule interactions. The dotted line represents the folding/unfolding curve, ● the gelation line for systems heated from the folded state. Different states are marked with capital letters A−D, and the lower case letters a, b, e and f represent the region of the state diagram represented by snapshot conformations in Figure 5.

The unfolding temperature for a 64-subunit homoglobule was followed as a function of increasing subunit volume fraction between 1% and 15%. The data for unfolding temperature vs V_F is included on the state diagram plots of Figures 3 and 4. The shape of the $T_{R,u}$ vs V_F plot depends on whether the globules are allowed to interact with each other or not. For the case where interglobule interactions are zero, $T_{R,u}$ increases relatively slowly with increasing V_F (Figure 3). This is a manifestation of the excluded volume effect. As V_F increases there is less space on the lattice for the globules to unfold and higher temperatures are required before unfolding occurs. The situation when the globules are allowed to interact attractively is different, however. In this case $T_{R,u}$ increases rapidly with V_F (Figure 4) and far faster than can be explained by excluded volume effects alone. We will show later that the reason for this is that the globules start to form aggregates at low volume fractions. These aggregates consist of two or more merged globules. In this state the globules behave as if they have more than 64 subunits. We have already seen that $T_{R,u}$ increases with increasing globule size (Figure 2), and this effect can explain the increase in $T_{R,u}$ with V_F observed in Figure 4.

Figures 3 and 4 are T_R vs V_F state diagrams for systems of interacting and noninteracting globules. Included on these state diagrams are the global unfolding temperature lines, gelation or crossover concentration lines, and, for the systems where

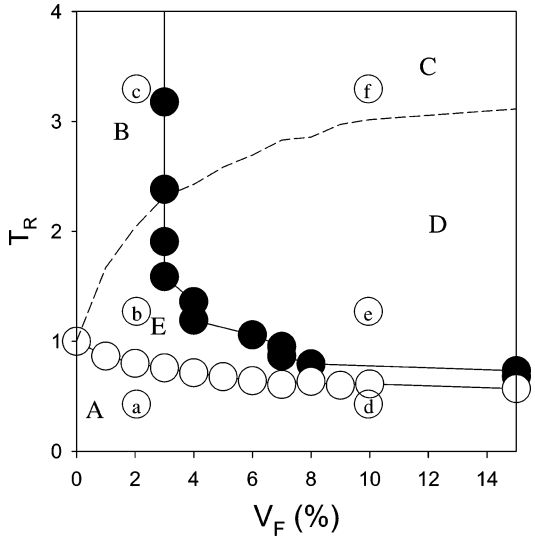

Figure 4. State diagram for homoglobules with interglobule attractive interactions. The dotted line represents the global folding/unfolding curve, ● the gelation line for systems heated from the folded state, and ○ the local unfolding line. Different states are marked with capital letters A−E, and the lower case letters a−f represent the region of the state diagram represented by snapshot conformations in Figure 6.

interactions are allowed between different globules (Figure 4), a local unfolding temperature line is also included. Four states can be defined in the state diagram of Figure 3 that are bounded by the crossover line and the unfolding temperature line. These are labeled A−D in Figure 3. State A is below the unfolding temperature and below the crossover concentration. In this state, any clusters that may occur are transient and not held together by attractive interactions but by entanglements between the globules. The molecules in this state are noninteracting folded globules. Figure 5a is a typical snapshot conformation of a system in this state corresponding to a T_R of 0.82 and a V_F of 2%. Increasing the temperature while maintaining the V_F at 2% leads to a transition to state B. State B is above the unfolding temperature but below the crossover concentration. Here the globules are unfolded and noninteracting. Figure 5b is a typical snapshot conformation for a system in state B corresponding to a T_R of 1.23 and a V_F of 2%. Holding the T_R constant at 1.23 and increasing the V_F to 10% results in a transition to state C (Figure 5e). In region C the temperature is above the unfolding temperature and V_F is above the crossover concentration. The structure of the region is that of an entangled polymer solution. Since there are no specific interactions between globules, any aggregates that form are the result of random entanglements between the chains. These will break and reform rapidly. It should be noted that since we vary V_F by keeping the number of globules constant and changing the size of the simulation box, the conformations at $V_F = 10\%$ represent a smaller volume than those at $V_F = 2\%$. The side length of the simulation box at $V_F = 2\%$ is 73 lattice sites, while at $V_F = 10\%$ this is 43 lattice sites. Thus, the globules for conformations at $V_F = 10\%$ appear larger in Figures 5, 6, 9, and 10. Lowering the temperature again at a constant V_F of 10%, the system moves into state D. State D is below the unfolding/refolding line but above the crossover concentration. Here a gel-like state is formed, but the globules are below the unfolding curve and therefore are folded or only partially unfolded. Figure 5d is a snapshot conformation of a system in state D at a V_F of 10% and $T_R = 0.82$. In this state the concentration of globules is high enough that they will interact with each other through excluded volume interactions, even though they remain folded. The molecular mobility of the globules decreases, and they become trapped in a solid-like state. The part of the gel line that is below the crossover line in Figure 3 may therefore correspond to a glass transition temperature, or even to a solid−liquid transition. If the temperature is increased above $T_R = 1.23$ to 3.27, then further unfolding of the globules occurs at both $V_F = 2\%$ (Figure 5c) and $V_F = 10\%$ (Figure 5f). In Figure 5f the system conformation also resembles that of a network gel.

The state diagram for interacting globules (Figure 4) differs from that for noninteracting homoglobules. In particular, a third line can be included on the plot that corresponds to a local unfolding transition. This line is absent from the state diagram for noninteracting globules. A second difference between Figures 3 and 4 is that in Figure 4 a fifth state (marked E on Figure 4) appears. The local unfolding and global unfolding lines and the gelation line bound this region. The gelation line in Figure 4 still resembles that found for experimental systems[5,32] and has a shape characteristic of a lower critical solution temperature (LCST) curve. Comparing the state diagrams for systems with and without interglobule interactions, we can see that the gelation line in Figure 4 has the same general form as the crossover line in Figure 3, but the critical gelation concentration (the concentration below which gelation does not occur) is shifted to lower V_F.

The structures found in the five states in Figure 4 differ from those found in Figure 3. In state A at V_F below the gelation concentration and T_R below both the global and local unfolding lines, the globules show some aggregation, but the individual globules maintain most of their "native" structure. Interaction between globules to form the aggregate is between their surfaces. Figure 6a is a typical snapshot conformation in this region at a V_F of 2% and a T_R of 0.49. In this conformation a number of small aggregates can be seen, the largest of which consists of five globules. The majority of globules (50%) still exist in a monomeric form in this state. As the temperature increases at a constant V_F, the system moves into state E. Here a number of individual globules aggregate to form larger oligomeric aggregates. The snapshot conformation in Figure 6b shows a system at 2% V_F and $T_R = 1.23$. The system in Figure 6b comprises two large aggregates containing 85 and 28 globules, two pentamers, and a dimer. In state E the structure of the individual globules becomes disordered as they interact and entangle with others in the oligomer. Thus, individual globules appear to unfold, while in fact they become part of larger, compact folded aggregate. These aggregates have a tendency to be elongated in form. State E may represent a phase-separated or microphase-separated state. Increasing the temperature further until the system is above the denaturation line (state B) leads to an unfolding of the larger aggregates. Figure 6c is a snapshot conformation for the system in state B at a V_F of 2% and a $T_R = 3.27$. In State B the large, compact elongated aggregates seen in state E have broken up to form a more diffuse structure. State B is above the global unfolding transition line, and the interactions are not strong enough to maintain the structure of the oligomeric aggregates. Consequently these unfold, leaving a system that contains random coils that interact weakly with each other to form small aggregates and some residual larger aggregates. These larger aggregates disappear as the temperature is increased further.

In all of states A, B, and E the V_F is below the critical gelation concentration and a percolating network is not formed. At higher V_F above the gelation line, structures can be formed that span the simulation box. At low temperature ($T_R = 0.49$) and a V_F

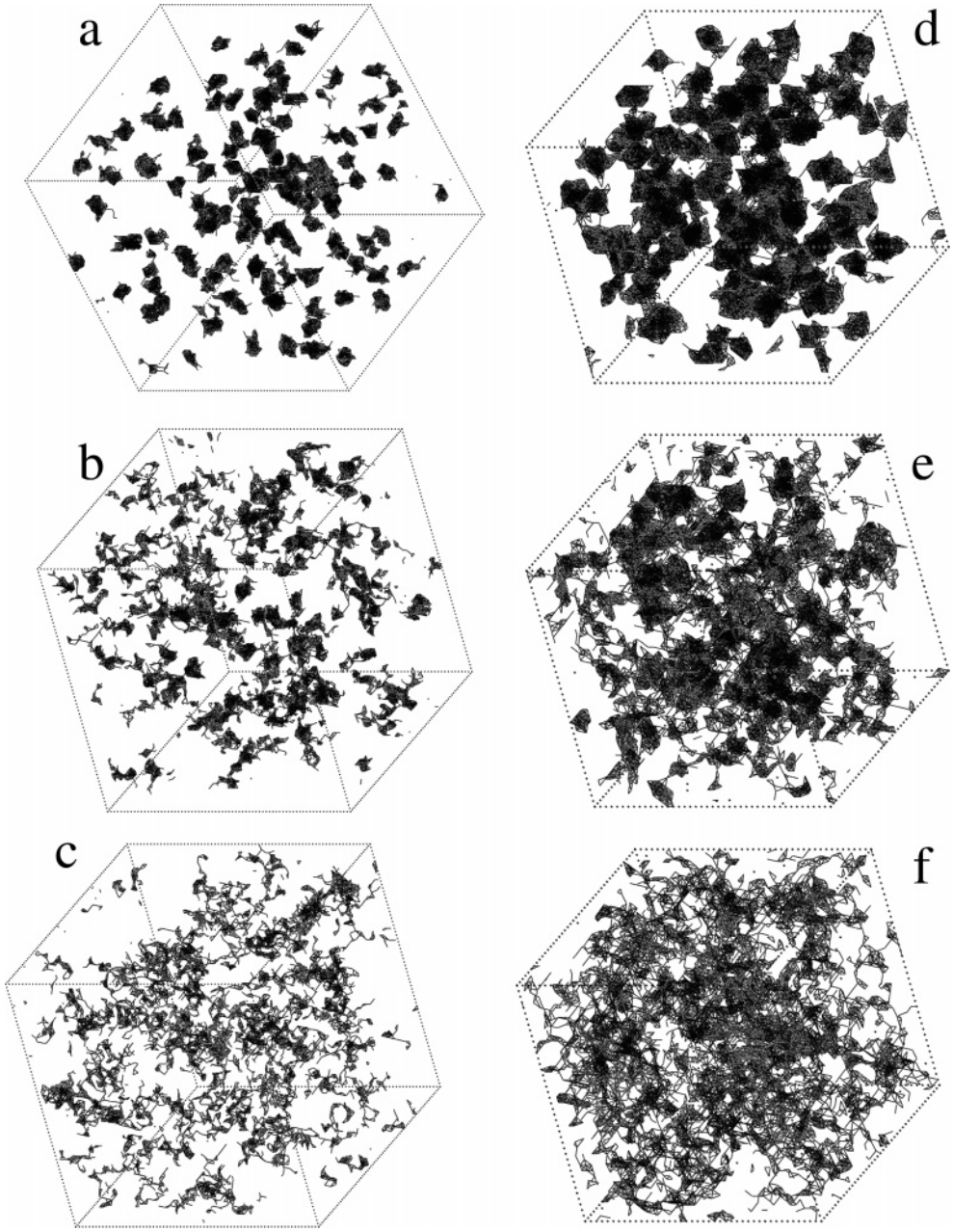

Figure 5. Snapshot conformations for noninteracting homoglobule systems from the state diagram in Figure 3. The following concentration/temperature combinations define the conformations. (a) $V_F = 2\%$, $T_R = 0.82$; (b) $V_F = 2\%$, $T_R = 1.23$; (c) $V_F = 2\%$, $T_R = 3.27$; (d) $V_F = 10\%$, $T_R = 0.82$; (e) $V_F = 10\%$, $T_R = 1.23$; (f) $V_F = 10\%$, $T_R = 3.27$. The box side lengths are 73 lattice sites for $V_F = 2\%$ and 43 lattice sites for $V_F = 10\%$.

of 10%, the system is below the gelation line but close to the local unfolding line. This system is still in state A. The snapshot conformation for this T_R/V_F combination (Figure 6d) shows that the system, as expected, does not form a percolating network, but there is significant aggregation of the globules into large oligomers. Some of these appear elongated in form since this system is close to the transition line between states A and E. If the temperature is increased to $T_R = 1.23$ at a V_F of 10%, the system enters state D. This state is below the global unfolding line but above the local unfolding line and the gelation line. Here elongated aggregates are formed, and these are joined together to form an open, heterogeneous network structure with large pores (Figure 6e). It is apparent from comparing Figures 6b and 6e that the elongated aggregate structure is conserved on increasing the V_F at a constant T_R. The form of the aggregates in state D is similar to that for state E, although the aggregate strands are thicker. Another feature shared by the aggregates in states D and E is the presence of highly elongated conformations of the globules, which act as bridges between the larger more dense aggregates. These bridges appear to be only one subunit thick and are composed of linear sequences of the subunits.

At higher temperatures above the denaturation line ($T_R = 3.27$), the gel structure in state D breaks down and a more homogeneous structure is formed (State C, Figure 6f). As the temperature is increased further, this begins to resemble the structure of state C in the state diagram for noninteracting homoglobules.

State Diagrams and Conformations of Heteroglobules. Figure 7 is the state diagram for heteroglobules where interglobule type 2 interactions are allowed, but not interglobule type 1 interactions, while the state diagram of Figure 8 is for systems where both type 1 and type 2 interglobule interactions are

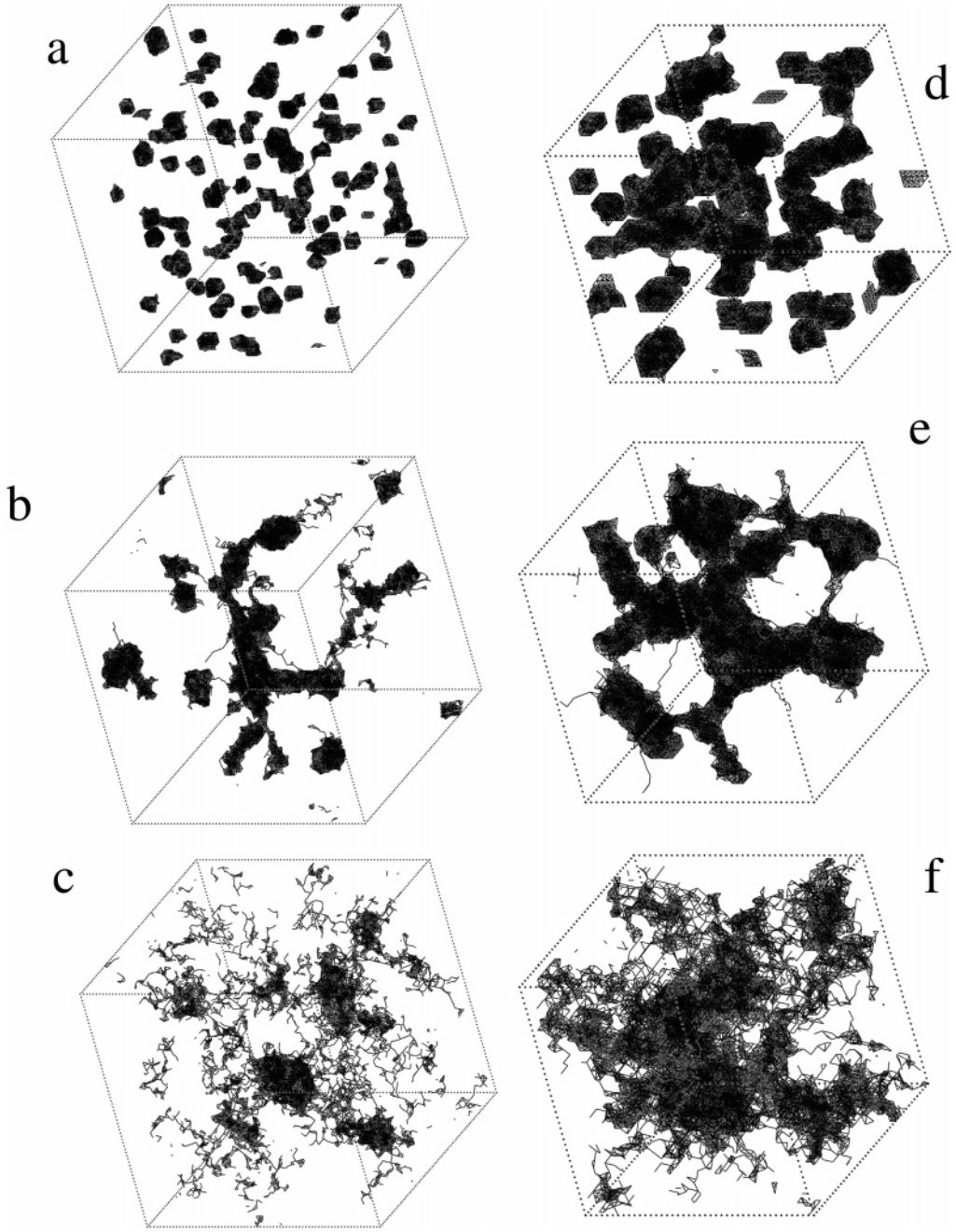

Figure 6. Snapshot conformations for interacting homoglobule systems from the state diagram in Figure 4. The following concentration/temperature combinations define the conformations. (a) $V_F = 2\%$, $T_R = 0.49$; (b) $V_F = 2\%$, $T_R = 1.23$; (c) $V_F = 2\%$, $T_R = 3.27$; (d) $V_F = 10\%$, $T_R = 0.49$; (e) $V_F = 10\%$, $T_R = 1.23$; (f) $V_F = 10\%$, $T_R = 3.27$. The box side lengths are 73 lattice sites for $V_F = 2\%$ and 43 lattice sites for $V_F = 10\%$.

allowed. The first point to note is that more states are found in these state diagrams than are observed for homoglobules. This is due to the presence of extra state boundaries that represent the local and global unfolding transitions of both type 1 and type 2 subunits.

The state diagram for systems with only type 2 interglobule interactions has six, maybe seven, states labeled A−G in Figure 7. Since there are no type 1 interglobule interactions in these systems, the global and local unfolding transitions for type 1 subunits occur at the same V_F/T_R combination. What is, perhaps, less expected is that the local unfolding transition line for type 2 subunits is also very close to the local and global unfolding transitions for type 1 subunits. The globule core, which is made up of only 16 type 2 subunits, is smaller than the rest of the globule made of 48 type 1 subunits. Therefore, the type 2 core of the globule will unfold at a lower temperature than the type 1 part of the globule. The combination of the proportion of type 2 subunits, and the relative strength of type 1 and type 2 interactions that we have chosen for these simulations leads to the local unfolding transitions of type 1 and type 2 subunits being close together in phase space. This suggests that by changing either the proportion of type 2 subunits, or the relative strength of the two subunit interactions (or both) we might be able to simulate systems and state diagrams with more than the six obvious states (A−F) seen in Figure 7. In fact there is some evidence in Figure 7 of a splitting of the local unfolding transitions for type 1 and type 2 subunits leading to a small seventh state labeled G. This is only observed once you move above the gelation/crossover line. In the state diagram where we have both type 1 and type 2 interglobule interactions

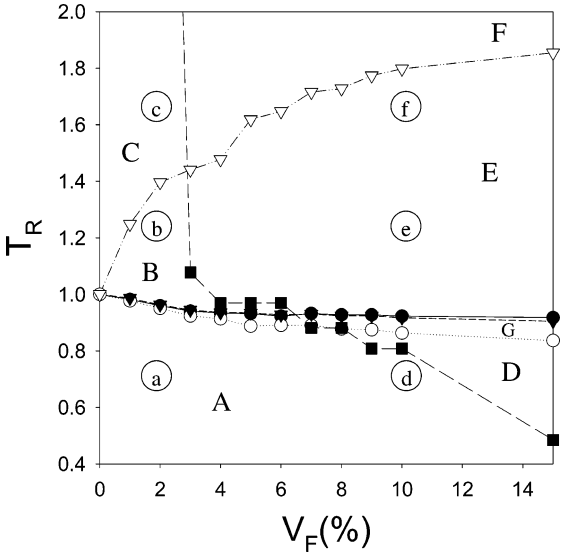

Figure 7. State diagram for heteroglobules without interglobule attractive interactions. ■ = the gelation/crossover line; ● = the local unfolding line for type 1 subunits; ○ = the local unfolding line for type 2 subunits; ▲ = the global unfolding line for type 1 subunits; △ = the global unfolding line for type 2 subunits. Different states are marked with capital letters A−G, and the lower case letters a−f represent the region of the state diagram represented by snapshot conformations in Figure 9.

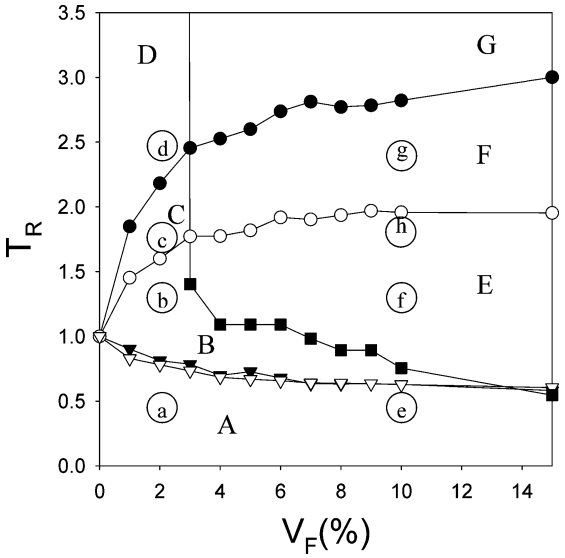

Figure 8. State diagram for heteroglobules with interglobule attractive interactions. ■ = the gelation/crossover line; ● = the local unfolding line for type 1 subunits; ○ = the local unfolding line for type 2 subunits; ▲ = the global unfolding line for type 1 subunits; △ = the global unfolding line for type 2 subunits. Different states are marked with capital letters A−G, and the lower case letters a−h represent the region of the state diagram represented by snapshot conformations in Figure 10.

(Figure 8), we also see that the local unfolding transitions for the two-subunit types are coincident. However, in this case they do not move apart at higher V_F to form an extra state.

Figure 9a is a snapshot conformation from state A in Figure 7, where $V_F = 2\%$ and $T_R = 0.7$. In state A, the system is below all of the unfolding transitions and below the gelation/crossover concentration line. The conformation is similar to those for state A in both Figures 3 and 4. Compared to the interacting homoglobules, the chance of aggregation in noninteracting heteroglobules is reduced since interaction can only be between exposed patches of type 2 subunits on the surface of the globule.

Transition from state A to state B in Figure 7 can be achieved by increasing the temperature to $T_R = 1.23$ at $V_F = 2\%$. Studying Figure 9b, the snapshot conformation for this state, reveals a number of features of this state. State B is above the local unfolding transitions, but below the global unfolding transition of the type 2 subunits and below the gelation/crossover line. Figure 9b shows that the outer layer of type 1 subunits has unfolded, and this has exposed the core of type 2 subunits. There are a number of aggregates in this system, although a gelled system has not formed. It appears that the type 2 subunits have aggregated together to form clusters that hold together the oligomers formed in this state, and may represent a micellar state. Increasing the temperature further to $T_R = 1.96$ at $V_F = 2\%$ leads to a transition into state C (Figure 9c). Here both the type 1 and type 2 subunits are unfolded, and the clusters of type 2 subunits have broken up (Figure 9c).

If we increase V_F to 10%, a similar trend is seen in the typical conformations found for states A, E, and F. At low $T_R = 0.7$, the system contains one large oligomer of 118 globules, a dimer, and 5 monomers (Figure 9d) and is in state A. The aggregates are formed by surface−surface contact between exposed type 2 subunits, or by random contact between type 1 or type 1 and 2 subunits. The level of clustering of the type 2 subunits is limited, probably because unfolding of the type 1 subunits must precede type 2 subunit cluster formation. An increase in temperature to $V_R = 1.23$ sees a transition to state E. In this state the conformation (Figure 9e) is similar to that for state B (Figure 9b). State E is characterized by the formation of a continuous network of subunits. The type 2 subunits cluster together, while the type 1 subunits are unfolded and form the continuous network. The type 2 clusters are not all joined together to form a continuous large aggregate, but are found as several separate smaller clusters. Therefore, in this state the system does not form a true physically linked gel, but it is closer to the structure of an entanglement type gel described above. This does suggest that at higher value of V_F we might see a true gelation line, where a continuous network of aggregated type 2 subunits is formed. This would lead to the existence of a further set of states at higher V_F that we have not been able to simulate in this investigation. Increasing the temperature further to $T_R = 1.96$, $V_F = 10\%$ allows the type 2 subunits to start unfolding, and the system, under these conditions in state F, forms an entanglement gel close in structure to that for the noninteracting homoglobules and heteroglobules under similar conditions. Some residual clustering of type 2 subunits is observed, but this disappears as the temperature is increased further.

We made brief mention above of a possible seventh state, marked G on Figure 7. It was not possible to study the structure of this state as none of our simulated combinations of V_F and T_R fell within this state.

The simulated equation of state for interacting heteroglobules (Figure 8) is even more complex than for the noninteracting heteroglobules. In Figure 8 the global unfolding transitions for both type 1 and type 2 subunits occur in a different place than the local unfolding transitions, and this leads to an extra state below the gelation line, a total of seven states. It should also be noted that in Figure 8 the local unfolding transitions of type 1 and 2 subunits is not separated at higher V_F to form an extra state (state G in Figure 7). If we look at the conformation of the system in state A (Figures 10a and 10e, $V_F = 2\%$ and 10%, $T_R = 0.49$), the structure is very similar to those for the noninteracting heteroglobules, with surface aggregated oligomers forming at both concentrations. Increasing the temperature to

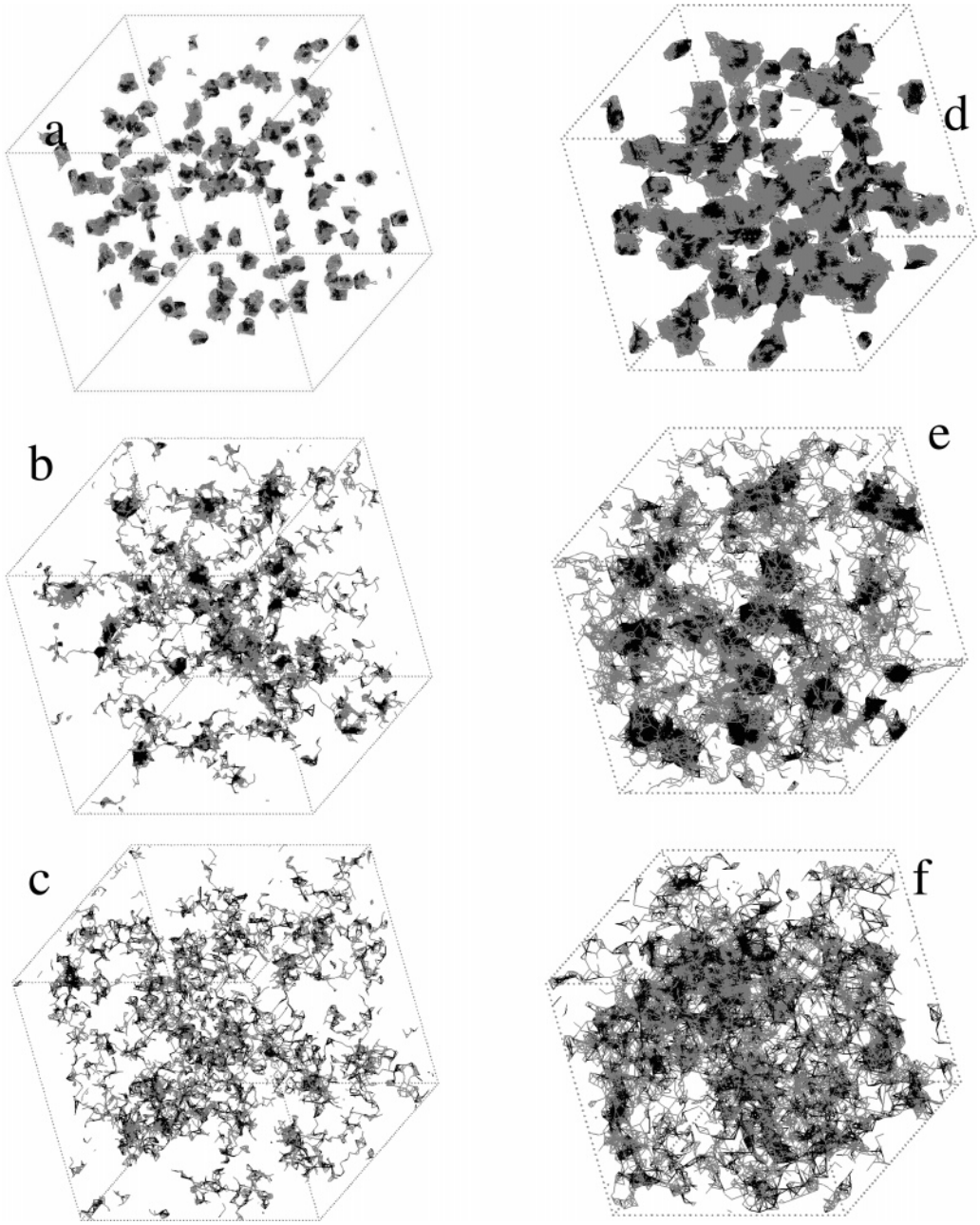

Figure 9. Snapshot conformations for noninteracting heteroglobule systems from the state diagram in Figure 7. The following concentration/temperature combinations define the conformations. (a) $V_F = 2\%$, $T_R = 0.7$; (b) $V_F = 2\%$, $T_R = 1.23$; (c) $V_F = 2\%$, $T_R = 1.96$; (d) $V_F = 10\%$, $T_R = 0.7$; (e) $V_F = 10\%$, $T_R = 1.23$; (f) $V_F = 10\%$, $T_R = 1.96$. The box side lengths are 73 lattice sites for $V_F = 2\%$ and 43 lattice sites for $V_F = 10\%$.

$T_R = 1.23$ we move into state B at 2% (Figure 10b) and state E (Figure 10f) at 10%. In these states we are above the local unfolding temperature but below the global unfolding temperature for both subunit types. The structure in these two states is noticeably different than the structure under the same conditions for noninteracting heteroglobules. For noninteracting heteroglobules, the type 1 subunits are unfolded and aggregation is via type 2 subunit cluster formation (Figures 9b and 9e). In contrast, for interacting heteroglobules aggregation is possible under these conditions via interaction between both type 1 and type 2 interactions, and the aggregates formed appear to be larger versions of a single globule, i.e., they appear to have a core of type 2 subunits surrounded by a layer of type 1 subunits. We also see the formation of elongated oligomers similar in structure to those observed under the same conditions for interacting homoglobules. If we increase the temperature to $T_R = 1.64$ at $V_F = 2\%$, we enter state C (Figure 10c). In this state, the type 2 subunit clusters have started to unfold (we are above the global unfolding transition for type 2 subunits) and they have a more random distribution within the globules. We also start to see some further unfolding of the type 1 subunit regions of the oligomers; however, since we are below the global unfolding line for type 1 subunits the aggregate structure is maintained, although they have a looser structure. Interestingly, if we keep the temperature at $T_R = 1.64$ and increase the system density to $V_F = 10\%$, we again move below the global unfolding line for type 2 subunits, and back into state E (Figure 10g), where a gelled system forms, with again clusters of type 2 subunits. If we return to $V_F = 2\%$ and increase the temperature further ($T_R = 2.46$, Figure 10d) the system moves into state D where both type 2 subunits now start to unfold globally. Again, however, if we increase the density to 10% V_F at the same temperature, we move back below the type 2 subunit global unfolding line and large aggregates reform (Figure 10h). At this

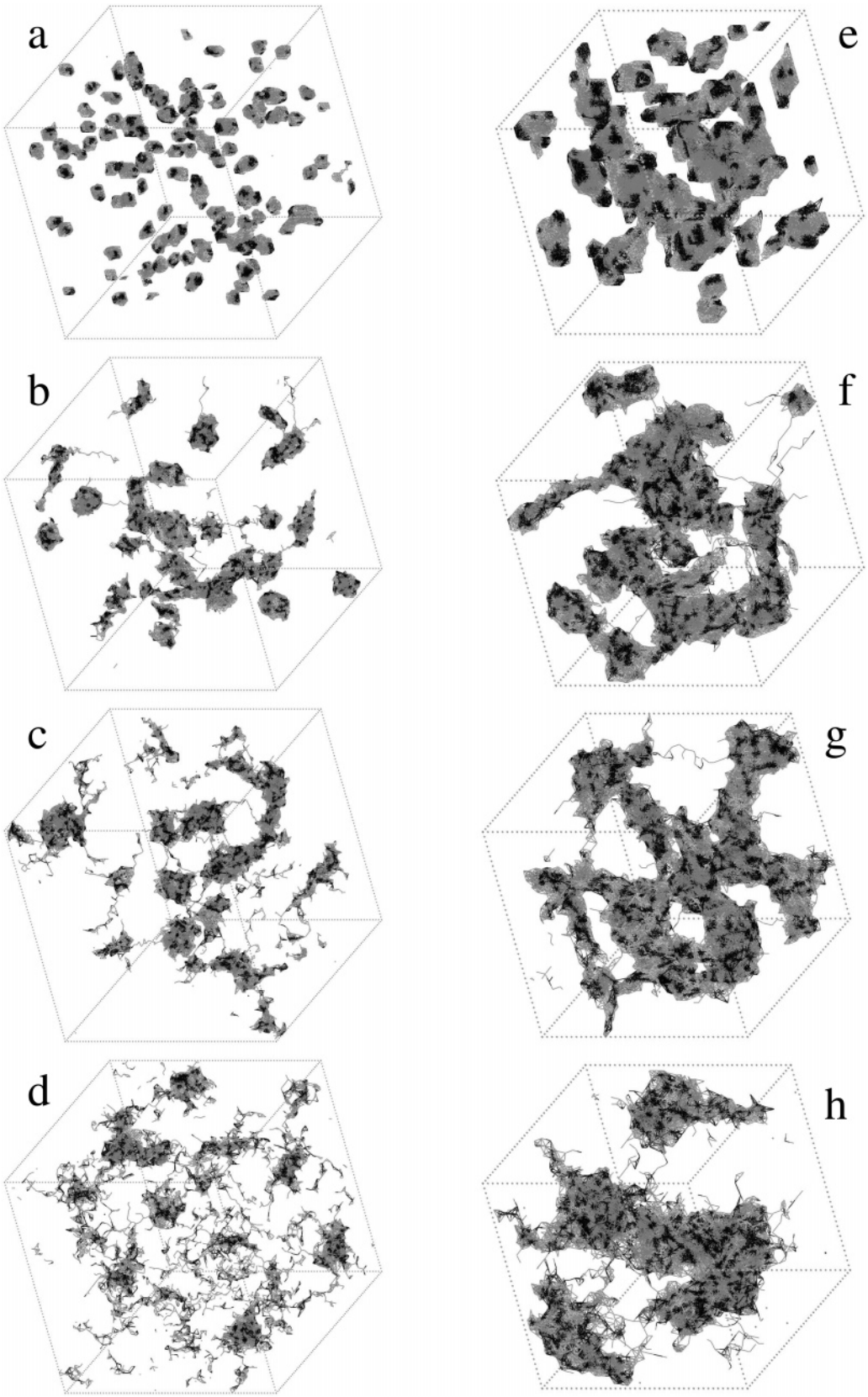

Figure 10. Snapshot conformations for interacting heteroglobule systems from the state diagram in Figure 8. The following concentration/temperature combinations define the conformations. (a) $V_F = 2\%$, $T_R = 0.49$; (b) $V_F = 2\%$, $T_R = 1.23$; (c) $V_F = 2\%$, $T_R = 1.64$; (d) $V_F = 2\%$, $T_R = 2.46$; (e) $V_F = 10\%$, $T_R = 0.49$; (f) $V_F = 10\%$, $T_R = 1.23$; (g) $V_F = 10\%$, $T_R = 1.64$; (f) $V_F = 10\%$, $T_R = 2.46$. The box side lengths are 73 lattice sites for $V_F = 2\%$ and 43 lattice sites for $V_F = 10\%$.

higher density, unfolding of both subunits occurs above a T_R of about 2.8, and the system enters state G (conformation not shown).

Analysis of Structure in Different Regions of the State Diagrams. Two methods have been used in an attempt to differentiate structural features in the various regions. Figure

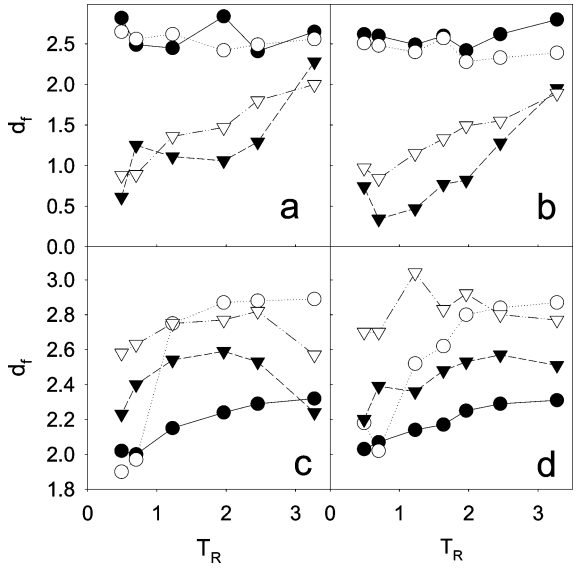

Figure 11. Fractal dimensions calculated at $V_F = 2\%$ and 10% for various values of T_R. (a) Homoglobule systems with d_f calculated according to the correlation between the centers of mass of the whole globules. (b) Heteroglobule systems with d_f calculated according to the correlation between the centers of mass of the whole globule. (c) Homoglobule systems with d_f calculated according to the correlation between the positions of individual subunits. (d) Heteroglobule systems with d_f calculated according to the correlation between the positions of individual subunits. For all four plots the following symbols apply. ● = noninteracting globules at $V_F = 2\%$; ○ = noninteracting globules at $V_F = 10\%$; ▼ = interacting globules at $V_F = 2\%$; ▽ = interacting globules at $V_F = 10\%$.

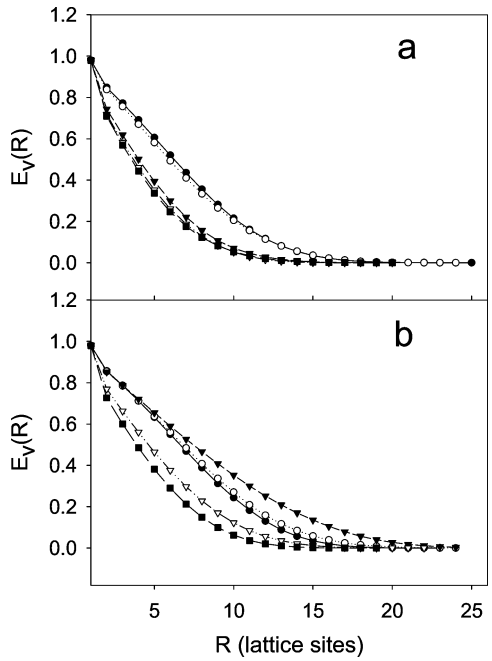

Figure 12. Plots of void exclusion probability for (a) noninteracting homoglobules at $V_F = 2\%$; (b) interacting homoglobules at $V_F = 2\%$. The following symbols apply for both plots (a) and (b): ● $T_R = 0.49$; ○ $T_R = 0.70$; ▼ $T_R = 1.23$; ▽ $T_R = 2.46$; ■ $T_R = 3.27$.

11 gives data for the fractal dimension calculated from eq 2 and Figure 12 the particle exclusion probability at V_F of 2% and 10% over a range of T_R including those shown in the snapshot conformations of Figures 5, 6, 9, and 10. It should be noted that the fractal dimension data are calculated over a relatively short range since the plots of $\log(N(r))$ vs $\log(r)$ usually became nonlinear over a short length scale. This is most noticeable at low T_R and/or low volume fraction where the linear region often only extends over the range of the radius of an individual globule. In practice, the radial distribution function for the systems was also calculated, but this proved to be a poor indicator of structure and the results are not included here.

If we look at the data for fractal dimension, some interesting trends can be discerned. For both noninteracting homo- and heteroglobules, scaling of the center of mass positions gives a fractal dimension in the region of 2.5−2.8 for all reduced temperatures (Figure 11a and 11b). This does not change as the V_F changes. At low T_R this probably reflects the compact nature of the individual globules and aggregates, while at higher T_R it suggests that the distribution of globules is relatively random and not ordered. For the interacting homo- and heteroglobules, the interesting feature is that the fractal dimension approaches 1 (or less than one in some cases) under some conditions. This suggests that the aggregates formed are linear. For the cases where d_f is less than one, this is an artifact most likely caused by the interpenetration of the globules, which would lead to the centers of mass being able to approach closer than would be possible for a hard sphere of equivalent radius. It is only at higher temperatures (and at V_F) that the fractal dimension approaches values that are typical of what would normally be called a fractal structure (i.e., in Figure 11 d_f is in the range 1.9−2.2 for both $V_F = 2\%$ and 10% at the highest reduced temperature of 3.27 for both interacting homo- and heteroglobules).

When the fractal dimension is calculated from the positions of all subunits in the system, the results give a range of fractal dimensions that are more typical of those measured for experimental gels. At low V_F (2%) for noninteracting homo- and heteroglobules, d_f starts at about 2.0 at low temperature and increases gradually to about 2.35 at the highest T_R as the globules unfold and start to interpenetrate and occupy a relatively greater volume of the simulation box. At a $V_F = 10\%$ at low T_R, the d_f for homo- and heteroglobule systems is still about 2%, but at the higher volume fraction d_f increases rapidly to about 2.9 once the globules start to unfold. These high values for d_f are not atypical of the values seen, for example, in globular protein gels and reflect the high volume occupancy of the molecules in these systems.

If we look at the interacting homo and heteroglobules a different trend is seen. For the interacting homoglobules at V_F of 2% d_f is about 2.2 at low T_R, increases to a maximum of 2.6 as T_R increases, and then decreases to 2.2 at the highest temperature. This reflects a change in the system from one where the globules are found in small aggregates, through a region of linear aggregation and finally at high T_R to an unfolded system. A similar trend is for interacting homoglobules at $V_F = 10\%$, but here the values of d_f at each T_R are higher because of the higher subunit density. The same trends are also observed for interacting heteroglobules, although in these systems the d_f does not go through a maximum and then decrease at high T_R. This would indicate that there is some residual densely packed structure probably in the form of only partially unfolded type 2 subunit regions. It should be noted that for the V_F/T_R combinations in Figures 13a and 13b, where d_f calculated from the centers of mass decreases to 1 or below, the same systems have a relatively high d_f when calculated from the positions of all subunits. While the overall globule adopts an ordered open aggregated arrangement, the individual subunits remain tightly packed together in the aggregates.

The accumulative void exclusion probability ($E(R)$) is another way of characterizing the structure of the systems. Figure 12 is

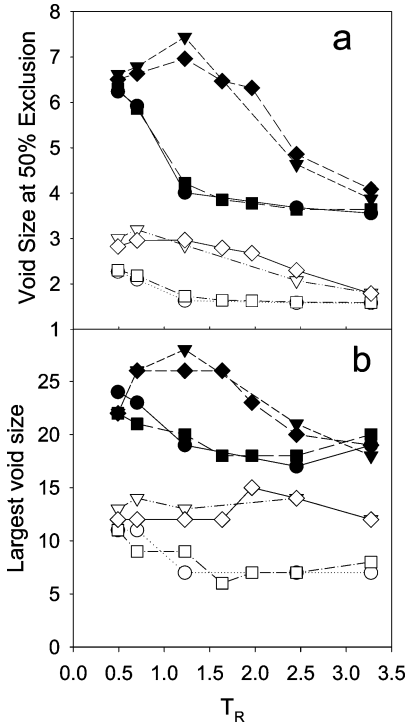

Figure 13. Plots of (a) void size at 50% exclusion probability; (b) largest void size both as a function of T_R. The following symbols apply on both graphs: ● noninteracting homoglobules at $V_F = 2\%$; ○ noninteracting homoglobules at $V_F = 10\%$; ▼ interacting homoglobules at $V_F = 2\%$; ▽ interacting homoglobules at $V_F = 10\%$; ■ noninteracting heteroglobules at $V_F = 2\%$; □ noninteracting heteroglobules at $V_F = 10\%$; ◆ interacting heteroglobules at $V_F = 2\%$; ◇ interacting heteroglobules at $V_F = 10\%$.

a typical set of $E(R)$ vs r data for the system of noninteracting and interacting homoglobules. In these data as the system moves across the unfolding line and/or the density increases the size of the void spaces in the system decreases. Rather than reproducing a series of curves for all the state diagrams, we have chosen to summarize the $E(R)$ date by calculating two representative parameters, the size of the particle at 50% exclusion and the maximum particle size that can be fitted into the simulation cell. These data are plotted in Figure 13. We can see from Figure 13 that the introduction of 25% type 2 subunits does not seem to have a great deal of effect on the void space sizes in the system. The data for both homo- and heteroglobules can be superimposed onto each other. The general trend for the pore size data is that for noninteracting hetero- and homoglobules the void size decreases as temperature increases, and as the V_F increases. This is most noticeable at V_F of 2%, while at $V_F = 10\%$ the void size is relatively insensitive to increasing temperature. For the interacting homo and heteroglobules it was also noticeable that at $V_F = 2\%$ the void size increased up to about $T_R = 1.2$ before decreasing. This corresponds to the region in the state diagrams where the extended linear aggregates are formed.

Discussion

Our simple homo- and heteroglobule models for unfolding and aggregation have produced a surprisingly large number of states in the state diagram. Some of these, such as network type entanglement gels and gels with elongated, fibrillar, aggregates have been observed in experimental systems. We should remember, however, that the conformations in these state diagrams are formed at relatively high reduced temperatures, whereas those from experimental studies on associating polymers, while they are heated to initiate gelation, are invariably cooled to around room temperature for further study. We have carried out some simulations on systems that are quench cooled from the athermal state ($\epsilon_s = 0$) to various lower temperatures. In these systems the position of the gelation line is shifted to lower temperatures. Thus, systems that are quench cooled to a particular temperature do seem to exhibit different conformations to those heated from the native state to the same temperature.

There are several regions in the state diagrams that show interesting features. In the state diagrams we observe elongated aggregates, and strands in regions D and E in Figure 4 for homopolymers, and in regions B and E in Figure 5 for heteropolymers. There are two possible mechanisms of formation of these structures, phase separation or gelation. It can be difficult to distinguish between these in simulation experiments. Gels are kinetically stable structures and persist over long time scales. Phase separating systems, however, while they may pass through a stage where the polymer phase forms a continuous network throughout the system, will ultimately demix into a thermodynamically stable equilibrium polymer and solvent phase in a relatively short time. Monte Carlo simulations are prone to slow approach to equilibrium for associating/aggregating polymer systems, and it is difficult to determine whether a slow approach to the equilibrium state is toward a gel or phase separated state.

Examination of the conformations for interacting homoglobules in state D (Figure 6e) and interacting heteroglobules in state E (Figure 10f) bear some resemblance to (2-D) micrographs of polymer systems undergoing spinodal decomposition.[27,33] It is also obvious, however, that these structures form a continuous network and thus they could equally be a gelled structure. If these structures are an intermediate en route to a phase-separated state, it is also conceivable that they may form via a nucleation and growth mechanism rather than spinodal decomposition. To distinguish between these two possible mechanisms we can look at the growth of aggregates in the systems with time. If we look at the aggregate size distribution as a function of time (number of MC steps, data not shown) for systems represented by Figures 6e and 10f, we do not see a growth of approximately equal-sized aggregates in the early stages of the simulation. Rather we see that one or two aggregates dominate the system even at short times. This is more characteristic of a nucleation and growth mechanism. It has also been observed that phase separation and gelation can be intimately related. In some cases, phase separating systems can enter a transient gel state, where a gel-like structure persists for a finite length of time before phase separation continues.[33] It is also possible for gelation to occur in a phase separating system so that the system becomes locked or pinned into a kinetically stable state.[22−27] It is possible that this occurs in our systems, where an initial phase separating system, probably by nucleation and growth, becomes trapped in a gelled state. It is interesting to point out that precisely this mechanism, nucleation and growth followed by network formation, has been proposed to explain the formation of fine-stranded protein gels under certain conditions in, for example, heat-denatured β-lactoglobulin solutions.[16,17]

A further interesting state occurs in the state diagram for noninteracting heteropolymers, where interaction occurs only between type 2 subunits. Here the globules can be thought of as being analogous to di-block copolymers that interact through one type of block. In this case the aggregates formed are micellar in structure; that is, they have a core of attractive subunits surrounded by a corona of noninteracting type 1 subunits, and the gelation line might better be described as a sol-to-micelle

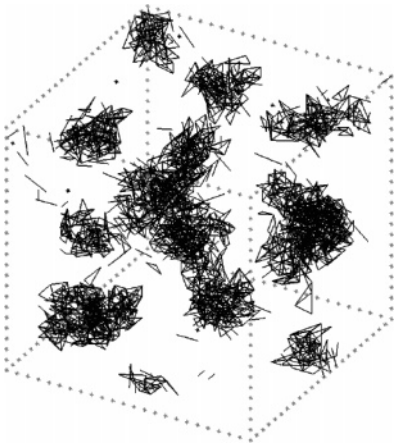

Figure 14. Snapshot conformation for noninteracting heteroglobule systems at $V_F = 58\%$, $T_R = 1.23$. For clarity all type 1 subunits have been removed and only type 2 subunits are shown.

transition line. Windle and co-workers[34] have carried out a detailed simulation study of block copolymers up to very high polymer volume fractions (about 80%). They observed that block copolymers could adopt a range of different mesophase structures depending on the strength of the interactions between associating blocks and the polymer volume fraction. They observed an interaction dependent micellar transition as the attractive interaction between the blocks increased, and a transition from compact micelles, to open worm-like micelles as the polymer concentration increased. On further increasing the concentration up to very high volume occupancies of the polymer, they observed that a number of different mesophases could form, depending on the interaction strength and the relative block size. These included the formation of hexagonal and lamella mesophases. We have used this approach in a previous study to investigate the micellization behavior of simulated casein proteins as a potential model for the structure and formation of the casein micelle in milk.[9,10] Our simulations have been successful in reproducing the micellar shapes that have been proposed for the four caseins types (α_{s1}-, α_{s2}-, β- and κ-casein).

In our simulations the formation of micellar structures at volume fractions of 2% and 10% and a T_R of 1.23 is obvious from Figures 9b and 9e. At $V_F = 10\%$ however, the concentration is too low for worm-like micelles to occur, and far to low for mesophase formation. We have extended the volume fraction to 58%, the highest density we are able to simulate in a reasonable time-scale using our methodology. Figure 14 is a snapshot conformation of a system at $V_F = 58\%$, $T_R = 1.23$. For clarity we have removed the type 1 subunits and only show the type 2 subunits. Here it is apparent that the micelles formed are elongated in form, and this may represent the onset of worm-like micelle formation.

Other simulation studies have also shown a range of aggregated states. Dima and Thirumalai[35] have used a more complicated heteropolymer model, with explicit representation of amino acid sequences, to model protein aggregation. They observe six different phases in the $T-V_F$ phase diagram, although they were unable to determine phase boundaries with any accuracy.[35] Most interesting was their observation of five distinct types of oligomeric aggregate. In our model we observe up to four aggregated states depending on whether we have homo- or heteroglobules, whether type 1 and type 2 subunits are folded or unfolded, and whether subunits are locally unfolded or not.

Giugliarelli et al.[36] have used a simple HP copolymer model (two subunit types hydrophobic and polar) to carry out a direct enumeration study of model protein aggregation. They observed three possible states in solution: a folded, native conformation, a folded (native) aggregated state, and an aggregated state where the protein had a changed geometric shape (unfolded). The latter state they considered as exhibiting prion-like behavior, where fibrillar aggregates are formed. While it may be premature to suggest that the elongated aggregates in our model represent an amyloid state, it is pertinent to point out the similarities between these aggregates and amyloid fibrils. The states where elongated aggregates are formed exhibit two features common to amyloid-like fibrils/fibrillar gels. The first of these features is that in the region of the state diagram where these structures are formed the fractal dimension (calculated from the globule center of mass) is close to 1 as observed for fibrillar β-lactoglobulin gels.[19] Second, the systems that form elongated aggregates are in a region of the state diagram below the global unfolding temperature. Thus they can be considered as only partially unfolded − a further condition that has been put forward for amyloid fibril formation.[37]

Our observation of a local unfolding temperature where individual globules unfold and merge to form larger aggregates has also been found by Cellmer et al.,[38] where they have noted a decrease in the melting temperature of aggregating lattice proteins. They attributed this to a domain swapping type mechanism.[39] Domain swapping occurs when two or more proteins exchange identical structural domains. It is accepted as a mechanism for protein self-assembly into quaternary structures and is believed to be a probable mechanism for protein aggregation in amyloid fibrils. In the latter, formation of intermolecular cross parallel β-sheet is believed to proceed via a domain swapping mechanism. Bratko and Bland[40] have shown that simulated aggregates formed by this type of mechanism from partially unfolded or misfolded molecules are more stable than the aggregates formed from chains in a native conformation. Thus domain swapping must lead to a lower free energy conformation than for aggregates of folded chains.

Quite why our homoglobule model prefers to form elongated aggregates, and ultimately to form elongated strands, is not certain. Khalatur et al.[41] have also noted the occurrence of elongated aggregates in molecular dynamics simulations of polyelectrolyte chains, but offer no explanation as to the mechanism of formation. We suspect that the individual globules tend to unfold into elongated chain-like conformations within each aggregate, and these align to form the oligomers. It is possible that the highly extended conformations (single subunit in diameter) we see in these systems (e.g., Figure 6b and e) act as templates for the formation of the extended aggregates. In other words, once these initial highly extended conformations are formed, other molecules become attached to them and they too become elongated, as this will then maximize interactions between the two molecules. Further globules will be added to the aggregates by the same mechanism. In our simulated conformations we have measured the separation of the two subunits in the globule that are furthest apart, and we do see an increase in this largest globule dimension for systems in the extended aggregate region of the state diagram, which supports this proposed mechanism of formation. Dima and Thirumalai[35] in their studies of protein-like heteropolymers found some sequences that are self-replicating. That is, an individual chain adopts a unique folded conformation and this acts as a template for other chains to aggregate onto, while at the same time adopting an identical conformation. The net effect is the

formation of a sheet-like structure of aggregated chains all with the same conformation. They suggest that this represents the formation of amyloid fibril type structures, where intermolecular β-sheet formation is believed to play a significant role in fibril formation. There is also evidence[42] that misfolded proteins can act as templates and induce misfolding and aggregation in other proteins. While our model does not have the complexity of amino acid sequence use in Dima and Thirumalai's work, it is conceivable that our simulated elongated conformations might also be considered as being formed via a very simple form of templating.

Conclusions

The phase behavior of associating polymers is complex and far from completely understood. In our simulations we see a range of possible states depending on the concentration of the globules, the temperature, and the relative degree of unfolding of the different subunit types. It is also possible that more gel-like states exist at higher V_F, in regions of the state diagram that we have not probed in this study. For associating polymers many aggregated structures can form such as gels, micelles, and mesophases. In associating biopolymers, micellar solutions and three gel states (entanglement, fibrillar/fine-stranded and particulate gels) can form. Our model appears to be able to produce most of these states, with the exception of mesophases and particulate gels. The lack of a particulate gel state is somewhat surprising given the highly compact nature of the aggregates in some of the states. It is possible that under the conditions used in our simulations the elongated aggregates we see are only stable at the relatively high temperatures where they are observed in the state diagram. If they are cooled from this state to a lower temperature they may phase separate into a particulate gel. This may suggest that the difference between fibrillar and particulate gels is a kinetic difference, and that given time the natural equilibrium state for any fine stranded gel network is to break down to a particulate gel.

Our model is a very simplistic representation of globular molecules. It does, however, reproduce some features that have analogues in protein gels. This suggests that at least some of these features arise from the globular nature of the molecules rather than the details of their sequence and interactions. We are still a long way from a comprehensive model for globular protein state behavior and gel structure. To achieve this requires a more sophisticated model. A refinement to the model would be to use a linear chain to represent the protein molecules. This would allow a more realistic representation of the primary sequence of the "protein", which would allow us to explore the effect of sequence and templating on the formation of fibrillar gels.

A thorough understanding and control of the mechanisms of protein gelation will allow the food scientist greater control over the structure and texture of manufactured foods. It may also lead to the intelligent design and construction of food gels that have novel textures. Taken to its logical conclusion, this would lead to the manipulation of gel structure through control of protein association, either by alteration of protein interaction forces or by selective design of protein sequences that give a particular gel type, structure, and texture. To achieve this will require the complementary approaches of experimentation and computer simulation.

Acknowledgment. The support of the Engineering and Physical Sciences Research Council (EPSRC Grant No. GR/R83481) in the form of a studentship for G.C. is gratefully acknowledged. Access to a Dell Poweredge Server through the Heriot-Watt University computer center is also acknowledged.

References and Notes

(1) Balsara, N. P. *Curr. Opin. Solid State Mater. Sci.* **1999**, *4*, 553.
(2) Bates, F. S.; Fredrickson, G. H. *Phys. Today* **1999**, *52*, 32−38.
(3) Gosal, W. S.; Ross-Murphy, S. B. *Curr. Opin. Colloid Interface Sci.* **2000**, *5*, 188.
(4) Norton, I. T.; Frith, W. J. *Food Hyd.* **2001**, *15*, 543.
(5) Tanaka, F. *Adv. Colloid Interface Sci.* **1996**, *63*, 23.
(6) Tanaka, F. *Physica A*, **1998**, *257*, 245.
(7) Tanaka, F. *J. Non Cryst. Sol.* **2002**, *307*−*310*, 688.
(8) Tanaka, F.; Koga, T. *Comput. Theor. Polym. Sci.* **2000**, *10*, 259.
(9) Euston, S. R. *Curr. Opin. Colloid Interface Sci.* **2004**, *9*, 321.
(10) Euston, S. R.; Horne, D. S. *Food Hyd.* **2005**, *19*, 379.
(11) Horne, D. S. *Int. Dairy J.* **1998**, *8*, 171.
(12) Horne, D. S. *Curr. Opin. Colloid Interface Sci.* **2002**, *7*, 456.
(13) Clark, A. H.; Kavanagh G. M.; Ross-Murphy, S. B. *Food Hyd.* **2001**, *15*, 383.
(14) Renkema, J. M. S. *Food Hyd.* **2004**, *18*, 39.
(15) Langton, M.; Hermansson, A. M. *Food Hyd.* **1992**, *5*, 523.
(16) Gosal, W. S.; Clark, A. H.; Pudney, P. D. A.; Ross-Murphy, S. B. *Langmuir* **2002**, *18*, 7174.
(17) Gosal, W. S.; Clark, A. H.; Ross-Murphy**,** S. B. *Biomacromolecules* **2004**, *5*, 2408.
(18) Zanuy, D.; Porat, Y.; Gazit, E.; Nussinov R. *Structure* **2004**, *12*, 439.
(19) Bromley, E. H. C.; Krebs, M. R. H.; Donald, A. M. *Faraday Discuss.* **2005**, *128*, 13.
(20) Gunton, J. D.; Miguel, M. S.; Sahni, P. S. In *Phase Transitions and Critical Phenomena*; Domb, C.; Lebowitz, J. L., Eds.; Academic Press: New York, 1983; pp 269−467.
(21) Binder, K. In *Phase Transformations in Materials*; Haasen, P., Ed.; VCH: Weinheim, 1991; pp 405−472.
(22) Miller, C. A.; Miller, D. *Colloids Surf.* **1985**, *16*, 219.
(23) Arnauts, J.; Berghmans, H. *Polym. Commun.* **1987**, *28*, 66.
(24) Hikmet, R. M.; Callister, S.; Keller, A. *Polymer* **1988**, *29*, 1378.
(25) Asnaghi, D.; Giglio, M.; Bossi, A.; Righetti, P. G. *J. Mol. Struct.* **1996**, *383*, 37.
(26) Kito, R.; Kaku, T.; Kubota, K.; Dobashi, T *Phys. Lett. A* **1999**, *259*, 302.
(27) de Hoog, E. H. A.; Tromp, R. H. *Colloids Surf. A* **2003**, *213*, 221.
(28) Euston, S. R.; Naser, Md. A. *Langmuir* **2005**, *21*, 4227.
(29) Dickinson, E.; Euston, S. R. *Adv. Colloid Interface Sci.* **1992**, *42*, 89. (b) Dickinson, E.; Euston, S. R. *J. Colloid Interface Sci.* **1992**, *152*, 562. (c) Dickinson, E.; Euston, S. R. *Food Hyd.* **1992**, *6*, 345.
(30) Stoddard, S. D. *J. Comput. Phys.* **1978**, *27*, 291.
(31) Dickinson, E. *J. Colloid Interface Sci.* **2000**, *225*, 2.
(32) Tobitani, A.; Ross-Murphy, S. B. *Macromolecules* **1997**, *30*, 4845.
(33) Verhaegh, N. A. M.; Asnaghi, D.; Lekkerkerker, H. N. W.; Giglio, M.; Cipelletti, L. *Physica A* **1997**, *242*, 104.
(34) Ding, J.; Carver, T. J.; Windle, A. H. *Comput. Theor. Polym. Sci.* **2001**, *11*, 483.
(35) Dima, R. I.; Thirumalai, D. *Prot. Sci.* **2002**, *11*, 1036.
(36) Giugliarelli, G.; Micheletti, C.; Banavar, J. R.; Maritan, A. *J. Chem. Phys.* **2000**, *113*, 5072.
(37) Uversky, V. N.; Fink, A. L. *Biochim. Biophys. Acta* **2004**, *1698*, 131.
(38) Cellmer, T.; Bratko, D.; Prausnitz, J. M.; Blanch, H. *J. Chem. Phys.* **2005**, *122*, article no. 174908.
(39) Yang, S.; Levine, H.; Onuchic, J. N. *J. Mol. Biol.* **2005**, *352*, 202.
(40) Bratko, D.; Blanch, H. W. *J. Chem. Phys.* **2001**, *114*, 561.
(41) Khalatur, P. G.; Khokhlov, A. R.; Mologin, D. A.; Reineker, P. *J. Chem. Phys.* **2003**, *119*, 1232.
(42) Malolepsza, E.; Boniecki, M.; Kolinski, A.; Piela, L *Proc. Nat. Acad. Sci. U.S.A.* **2005**, *102*, 7835.